Validation of Emulated Omnidirectional Antenna Output Using Directive Antenna Data

Hejselbæk, Johannes; Karstensen, Anders; Nielsen, Jesper Ødum; Fan, Wei; Pedersen, Gert F.

Published in:
2017 11th European Conference on Antennas and Propagation (EuCAP)

DOI (link to publication from Publisher):
10.23919/EuCAP.2017.7928192

Publication date:
2017

Document Version
Accepted author manuscript, peer reviewed version

Validation of Emulated Omnidirectional Antenna Output Using Directive Antenna Data

Johannes Hejselbæk, Anders Karstensen, Jesper Ødum Nielsen, Wei Fan, Gert Frølund Pedersen
Antennas, Propagation and Radio Networking section, Department of Electronic Systems, Aalborg University, Denmark
E-mail: {joh, andka, jni, wfa, gfp}@es.aau.dk

***Abstract*—In this paper, we present validation of a method for constructing a virtual omnidirectional antenna in the azimuth plane. The virtual omnidirectional antenna utilizes a combination of data from directive horn antennas. The aim is to utilize the high gain of the horn antenna to improve the dynamic range of channel sounding measurements conducted in the centimeter and millimeter wave bands. The resulting complex impulse response from the virtual omnidirectional antenna is used to find the power-delay-profile (PDP). This is then compared to measurements conducted at the same time using a real omnidirectional antenna. The validation shows that the synthesized omnidirectional is capable of predicting main components and the slope of the PDP. Further, it is shown that by choosing angular sampling steps corresponding to the half power beam width (HPBW) of the used antenna similar power levels can be achieved.**

***Index Terms*—millimetre-wave, centimetre-wave, channel measurement, channel sounding, power-delay-profile, virtual omnidirectional antenna, synthesized omnidirectional antenna.**

I. Introduction

Lately, there has been a great interest in channel measurements of the centimeter and millimeter wave bands [1]–[3]. This is a part of the process of moving towards fifth-generation cellular networks (5G) [4]. To develop statistical channel models for 5G, measurements in different scenarios have to be conducted. The proposed use of centimeter and millimeter wave bands introduces high path-losses. To overcome this, high-gain antennas are often used in measurements. The high-gain antennas are highly directive and often of the horn type. To express power at a given point for use in omnidirectional path-loss models, this directivity of the used antenna is unwanted. Due to this, synthesizing techniques have been applied to create virtual omnidirectional antennas [5]–[9]. The approach of synthesizing with directional elements is not new, as shown by [10], [11]. However, the recent measurement endeavors have rekindled interest.

This paper presents a validation of a method for creating a virtual omnidirectional antenna in the azimuth plane. The virtual omnidirectional antenna is synthesized using data from a directive horn. The performance of the synthesizing is then compared with measurements of the power-delay-profile (PDP) conducted at the same time with a real omnidirectional antenna. Further, it is investigated what impact the choice of angular sample density has on the synthesized PDP.

The paper is organized as follows. Section II describes the measurement setup used for the validation. Section III elaborates the synthesizing technique. Section IV presents the recorded channel impulse responses and the comparison between synthesized and real omnidirectional measurements. Section V summarizes this work.

II. Validation Measurement

The measurement used for this validation was conducted as a part of measurement campaign in a laboratory environment. The measurement surroundings are shown in Fig. 1.

Fig. 1. View of the laboratory where the measurement was conducted.

A VNA based measurement system as described in [12] has been used for the measurement campaign. The transmit side (TX) is a horn antenna (Pasternack - PE9851/2F-10). The receive side (RX) is using both a horn (Flann - 22240-20) and a bi-conical antenna (AINFO - SZ-2003000/P). The VNA system is capable of recording both complex frequency responses from the two RX antennas using two test mixers.

The specific parameters of the system are presented in TABLE I.

In Fig. 2, the position of the transmitter (TX) and receiver (RX) is marked in relation to the surroundings. There are two RX positions, RX-1 in clear line-of-sight (LOS) and RX-2 in non-line-of-sight (NLOS).

The TX antenna was oriented towards position RX-1 in a height of 100 cm. The bi-conical antenna was placed at the same height as the TX antenna in the rotation center of the turntable. The horn antenna was placed below the bi-conical antenna, orthogonal to the rotation axis, in a height of 90 cm. The starting orientation of the horn antenna point to the south as marked in Fig. 2. The horn antenna is rotated clockwise in steps of 1°. A Complex Impulse Response (CIR)

TABLE I
MEASUREMENT SYSTEM DETAILS

Parameter	Setting
Center Frequency	28 GHz
Bandwidth	4 GHz
Frequency Points	1500
TX power	15 dBm
TX antenna Azimuth HPBW	54°
TX antenna Elevation HPBW	53°
TX antenna gain	10 dBi
RX horn antenna Azimuth HPBW	22°
RX horn antenna Elevation HPBW	21°
RX horn antenna gain	18 dBi
RX bi-conical antenna gain	6 dBi

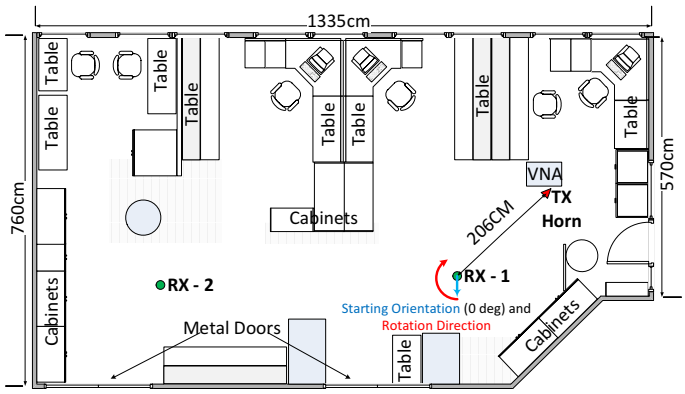

Fig. 2. Positioning of transmitter and turntable with receiving horn and bi-conical antenna.

is recorded for both horn and bi-conical antenna for each rotation step. One complete scan of the azimuth plane took roughly 6 minutes in which the scenario where completely static.

III. SYNTHESIZING METHOD

The common model for the CIR in the stationary case is expressed as Eq. 1 which follows [13]. The simplified model, in Eq. 1, can be expanded to include the impact of the antennas orientation as shown in Eq. 2.

$$h(\tau) = \sum_{k=1}^{K} a_k \, \delta\left(\tau - \tau_k\right) \, e^{j\varphi_k} \tag{1}$$

$$h(\tau, \phi) = \sum_{k=1}^{K} a_k \, \delta\left(\phi - \phi_k\right) \delta\left(\tau - \tau_k\right) \, e^{j\varphi_k} \tag{2}$$

where K is the total number of resolvable multipath components (MPC). a_k, τ_k, ϕ_k and φ_k are respectively the amplitude, arrival time, direction and phase for the kth component.

In practice the measurement system does not have infinite bandwidth and the used antenna will have a given beamwidth. Therefore, instead of $\delta(\cdot)$, the following will use $p(\tau)$ to describe the pulse shape and $A(\phi)$ will describe the antennas radiation pattern. The resulting expression follows the one presented in [7].

$$h_l^d(\tau) = \sum_{k=1}^{K} A\left(\phi_k - \phi_l^o\right) \, G_k \, p\left(\tau - \tau_k\right) \tag{3}$$

where h_l^d is the directive CIR to a given direction, l. The complex radiation pattern for the used antenna is expressed by $A\left(\phi_k - \phi_l^o\right)$, where ϕ_k is direction of the incoming k'th component and ϕ_l^o is the orientation of the antenna for the l'th direction. G_k express the complex gain of the k'th component as $G_k = a_k \, e^{j\varphi_k}$.

Note that in this paper only the azimuth plane is investigated. Therefore, the complex radiation pattern function A is only dependent on the azimuth angle (ϕ) and not the elevation angle (θ).

Using Eq. 3 an approximation of the CIR for an omnidirectional antenna in the azimuth plane can be obtained with a summation of L responses distributed over a full rotation of the horn antenna. However, as the measurement system records a CIR for each direction (l), each CIR will include minor errors due to the nature of the measurement system. This error will present itself as small random amplitude and phase variations (V_l,v_l) and additive noise (w_l). Due to this, these are added in the approximation shown in Eq. 4.

$$h^o(\tau) = \sum_{l=1}^{L} h_l^d(\tau) \, V_l e^{jv_l} + w_l(\tau) \tag{4}$$

where $h^o(\tau)$ is the approximated omnidirectional CIR.

The purpose of approximating the omnidirectional CIR is to be able to find the omnidirectional PDP for the measurement location. The PDP is found as shown in Eq. 5.

$$P(\tau) = |h^o(\tau)|^2 \tag{5}$$

In Eq. 6, Eq. 5 is expanded and Eq. 3 is substituted into Eq. 4. The random amplitude variations (V_l) and additive noise (w_l) from the measurement system is assumed to be insignificant compared to the measured channel response and therefore ignored here.

$$\begin{aligned} P(\tau) &= \sum_{l=1}^{L} \sum_{l'=1}^{L'} \sum_{k=1}^{K} \sum_{k'=1}^{K'} A\left(\phi_k - \phi_l^o\right) \, G_k \, p\left(\tau - \tau_k\right) \\ &\quad A^*\left(\phi_{k'} - \phi_{l'}^o\right) \, G_{k'}^* \, p^*\left(\tau - \tau_{k'}\right) \, e^{j(v_l - v_{l'})} \qquad (6) \\ &= \sum_{k=1}^{K} \sum_{k'=1}^{K'} \left[\sum_{l=1}^{L} A\left(\phi_k - \phi_l^o\right) e^{jv_l} \right] G_k \, p\left(\tau - \tau_k\right) \\ &\quad \left[\sum_{l'=1}^{L'} A^*\left(\phi_{k'} - \phi_{l'}^o\right) e^{-jv_{l'}} \right] G_{k'}^* \, p^*\left(\tau - \tau_{k'}\right) \qquad (6a) \end{aligned}$$

where the two terms dependent on the measurement of each direction (l) is contained by the brackets in Eq. 6a.

Following the approach presented in [7], it is assumed that the phase error (v_l) of the measurements within the beamwidth of the used horn antenna is approximately constant. Further,

it is assumed that the increments of ϕ_l^o is small compared to the beamwidth of the used horn antenna. The result of these assumptions is an approximation of the antenna and phase error term as shown in expression Eq. 7.

$$\sum_{l=1}^{L} A\left(\phi_k - \phi_l^o\right) e^{jv_l} \simeq c\, e^{jv_k} \tag{7}$$

where c is the constant determined by the radiation pattern of the used horn antenna. The phase error is now included in the random variable v_k. Note the transform from l to k. This is a result of the seeing the phase error as effectively distorting the individual MPC.

The approximation in (7) is used to replace the bracket part of Eq. 6a as shown in Eq. 8.

$$P(\tau) \simeq \sum_{k=1}^{K} \sum_{k'=1}^{K'} |c|^2 e^{j(v_k - v_{k'})} G_k G_{k'}^* p\left(\tau - \tau_k\right) p^*\left(\tau - \tau_{k'}\right) \tag{8}$$

As stated, the approximation requires the measurement of the angular plane is sufficiently dense. Due to this the effect of choosing different increments of ϕ_l^o and thereby the number of directions (L) is studied in the following section.

IV. Results

The measured power-angle-delay profile (PADP) using the horn antenna are shown in Fig. 3 and Fig. 4 for line-of-sight (LOS) and non-line-of-sight (NLOS), respectively.

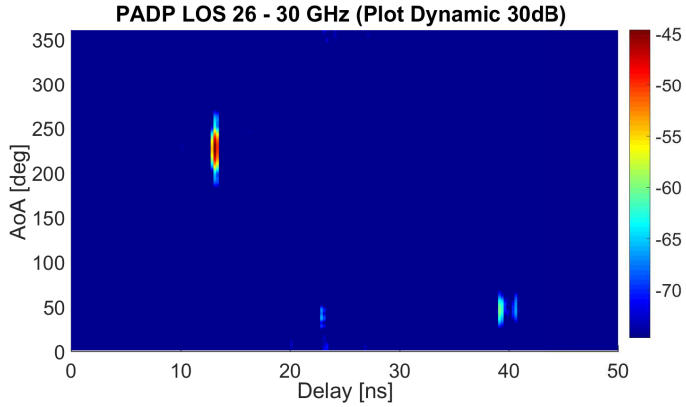

Fig. 3. Measured power-angle-delay profile for the LOS measurement

A. Emulated Omnidirectional PDP

Using the measured data from the horn antennas, the omni-directional PDP is approximated using (5) and compared to the measured data from the bi-conical antenna. The approximation is done using different increments of ϕ_l^o. In specific 1, 5, 10 and 20 degrees which are all within the HPBW of the used horn antenna of 22°. To enable comparison of the shape of the PDPs they are normalize to the maximum power (main component).

The comparison for the LOS measurement is shown in Fig. 5. Here it can be noted that the approximation using different

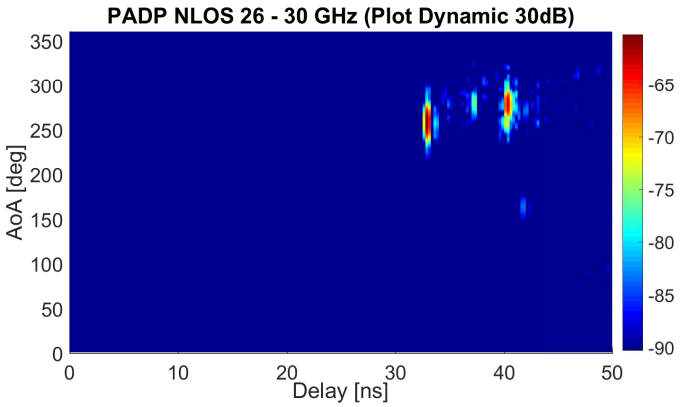

Fig. 4. Measured power-angle-delay profile for the NLOS measurement

increments show close to no difference. To highlight the differences utilizing different angular increments, a zoomed version in shown in Fig. 6.

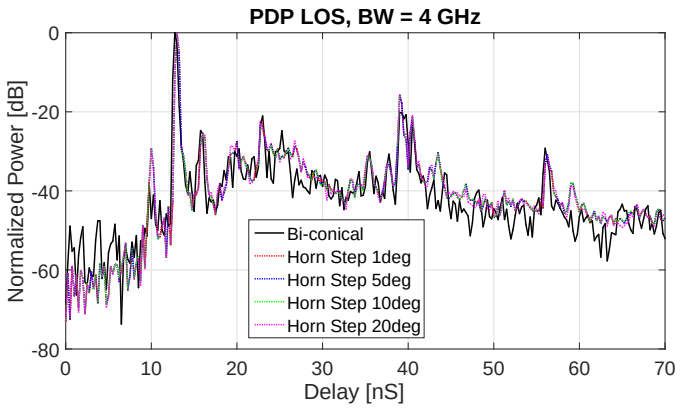

Fig. 5. PDP for the LOS comparison

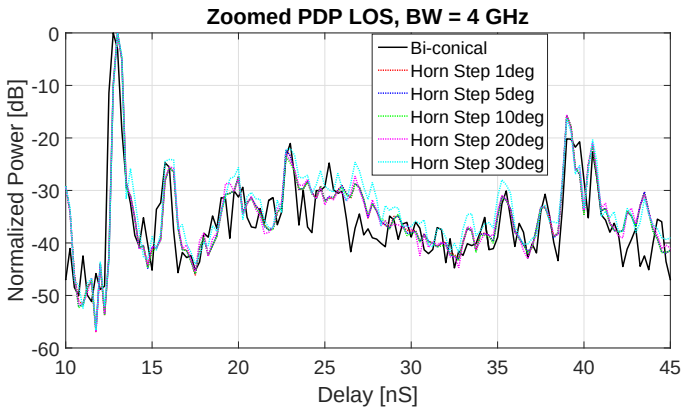

Fig. 6. Zoomed PDP for the LOS comparison

In the zoomed version shown in Fig. 6, an approximation using increments of 30° is also included. This trace (cyan) starts to deviate from the other approximations. This is a result of the angular spectrum now is starting to be under sampled compared to the HPBW of the used horn antenna.

Investigating the details of Fig. 5 and Fig. 6 shows that the main component of the bi-conical PDP and the approximated PDP is offset by 0.25ns in the delay domain. Using the geometric relation this can be explained by the small height difference of the bi-conical antenna and the horn antenna.

The comparison for the NLOS measurement is shown in Fig. 7 together with a zoomed version in Fig. 8.

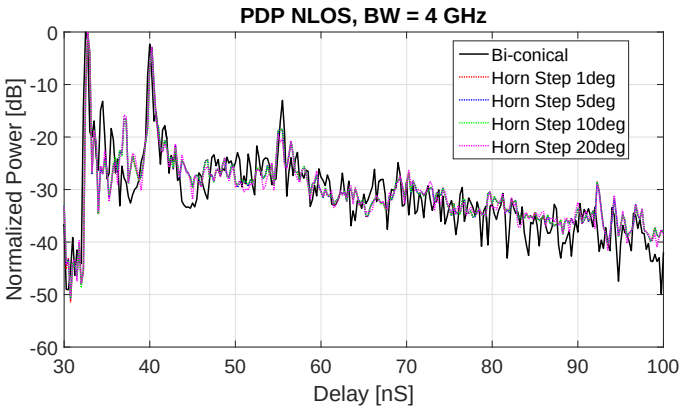

Fig. 7. PDP for the NLOS comparison

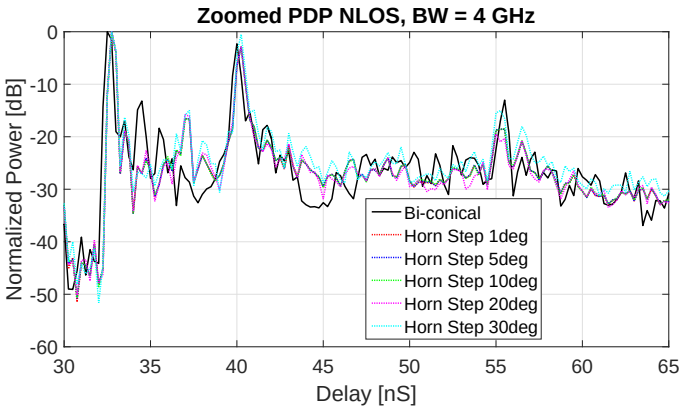

Fig. 8. Zoomed PDP for the NLOS comparison

The two plots show that the approximation for the NLOS case also is capable of capturing the dominant components and follow the general slope of the PDP. However, there are two components at approximately 34ns and 36ns which are not captured. Instead, the approximation shows a component at approximately 37ns. The delay offset between the main component of the bi-conical PDP and the approximated PDP is again 0.25ns.

B. Large Angular Spread

The lack of significant difference between the approximations using 1, 5, 10 and 20 degrees angular increments could be explained by the very directional measurement data. Due to this a PADP with a larger angular spread have been constructed. This is constructed by editing the NLOS measurement and copying the response between 225° and 325° to 25° and 125° and offsetting it by 10ns. The resulting PADP is shown in Fig. 9.

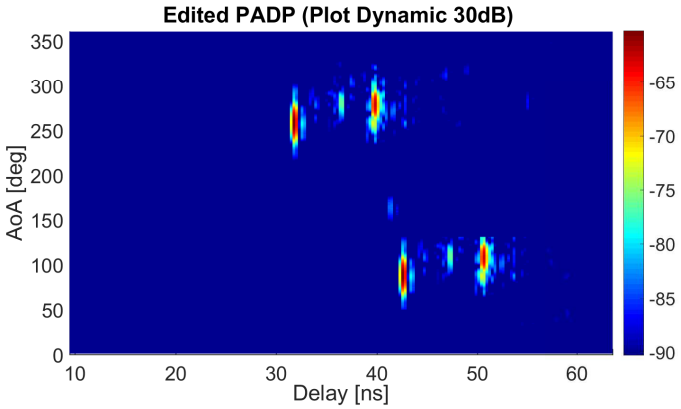

Fig. 9. Edited power-angle-delay profile

The PDP have, as in the previous, been approximated using different angular increments as shown in Fig. 10. It is not possible to compare the approximations to the bi-conical antenna as this is based on an edited PADP. It is however still possible to compare the approximations which show that they are close to overlapping, as in the previous comparisons. Only significant deviations are seen from the increments of 30° (cyan). This indicates that as long as the angular increments are below the HPBW of the used horn antenna the approximation shows good agreement with the measured reference.

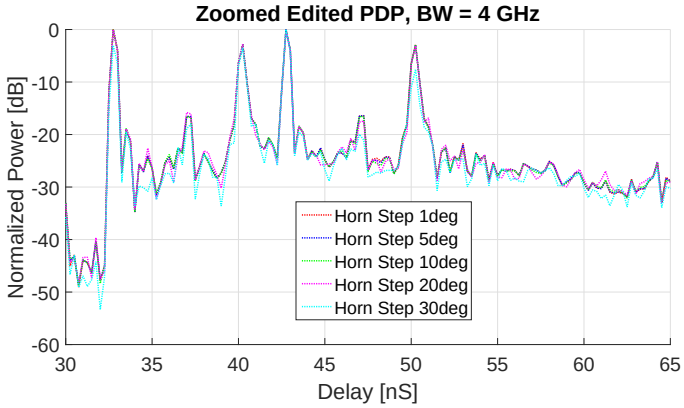

Fig. 10. Zoomed PDP for the edited PDP comparison

C. Power Estimation

In the previous sections, the power has been normalized to the maximum power (main component), as the aim was to compare the shape of the PDP. If the aim is to compare the absolute power value for the measurement point, this normalization should be removed. Instead, the power levels have been scaled with the antenna gains as shown in TABLE I. The resulting PDP for the bi-conical measurement data is presented in Fig. 11 together with the approximations using different angular increments.

Fig. 11 shows that using small angular increments when sampling the azimuth plane will result in a overestimated power. This is a result of the same components being captured more than once by the broader beam of the antenna and

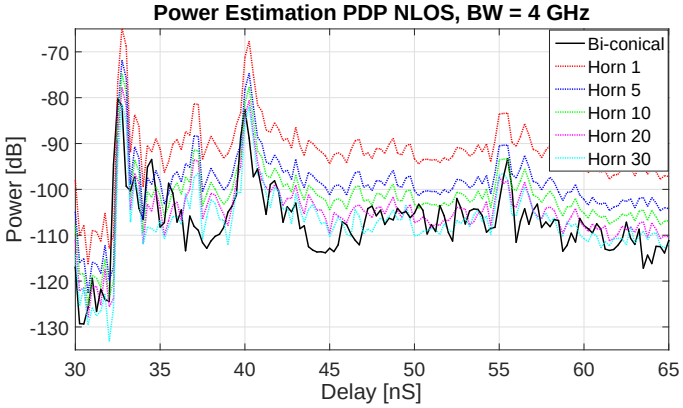

Fig. 11. Comparison of the unnormalized power levels using the different approximations

included multiple times as seen from Eq. 7. A solution could be to scale the summation of power accordingly to the number of samples within a given beamwidth. This relates to the assumptions made in [5], [6], [8] where angular increments corresponding to the HPBW is chosen. The reason for this is to avoid the 'overlapping' of the most significant part of the radiation pattern. When investigating Fig. 11 it is also seen that by using increments comparable to the HPBW of the used horn (22°) the power levels are quite well predicted.

V. Conclusion

This paper presents a validation of a method for approximating the omnidirectional PDP using measurement data from directional horn antennas in the azimuth domain. Measurements using an omnidirectional bi-conical antenna and a directional horn antenna have been conducted at the same time and location. The measurement data from the bi-conical antenna have been used as a reference for comparison of approximations based on the measurement data from the directional horn. It is shown in the paper that it is possible to approximate the omnidirectional PDP. The paper also shows that changing the angular increments of the horn antenna have a small impact on the approximation as long as the increments are chosen smaller or equivalent to the HPBW of the used horn antenna. Finally, it is shown that choosing angular increments of the horn antenna equivalent to the HPBW will enable estimation of the power levels with good agreement to the reference measurement.

Acknowledgment

The work has been conducted under the framework of the VIRTUOSO project. The Danish National Advanced Technology Foundation supports this project.

References

[1] T. Rappaport, S. Sun, R. Mayzus, H. Zhao, Y. Azar, K. Wang, G. Wong, J. Schulz, M. Samimi, and F. Gutierrez, "Millimeter wave mobile communications for 5g cellular: It will work!" *Access, IEEE*, vol. 1, pp. 335–349, 2013.

[2] T. Rapport, F. Gutierrez, E. Ben-Dor, J. Murdock, Y. Qiao, and J. Tamir, "Broadband millimeter-wave propagation measurements and models using adaptive-beam antennas for outdoor urban cellular communications," *IEEE Transactions on Antennas and Propagation*, vol. 61, pp. 1850–1859, April 2013.

[3] W. Fan, I. C. Llorente, J. Ødum Nielsen, K. Olesen, and G. F. Pedersen, "Measured wideband characteristics of indoor channels at centimetric and millimetric bands," *EURASIP Journal on Wireless Communications and Networking*, vol. Pre Press, no. Special issue on Radio Channel models for higher frequency bands, 2016.

[4] J. G. Andrews, S. Buzzi, W. Choi, S. V. Hanly, A. Lozano, A. C. K. Soong, and J. C. Zhang, "What will 5g be?" *IEEE Journal on Selected Areas in Communications*, vol. 32, no. 6, pp. 1065–1082, June 2014.

[5] S. Hur, Y.-J. Cho, J. Lee, N.-G. Kang, J. Park, and H. Benn, "Synchronous channel sounder using horn antenna and indoor measurements on 28 ghz," in *Communications and Networking (BlackSeaCom), 2014 IEEE International Black Sea Conference on*, May 2014, pp. 83–87.

[6] J. Liang, J. Lee, M. D. Kim, and X. Yin, "Synthesis techniques of narrow beam-width directional antenna measurements for millimeter-wave channel characterization," in *Information and Communication Technology Convergence (ICTC), 2015 International Conference on*, Oct 2015, pp. 689–693.

[7] J. . Nielsen and G. F. Pedersen, "Dual-polarized indoor propagation at 26 ghz," in *2016 IEEE 27th International Symposium on Personal, Indoor and Mobile Radio Communications*, September 2016.

[8] S. Sun, G. R. MacCartney, M. K. Samimi, and T. S. Rappaport, "Synthesizing omnidirectional antenna patterns, received power and path loss from directional antennas for 5g millimeter-wave communications," in *2015 IEEE Global Communications Conference (GLOBECOM)*, Dec 2015, pp. 1–7.

[9] K. Haneda, S. L. H. Nguyen, J. Järveläinen, and J. Putkonen, "Estimating the omni-directional pathloss from directional channel sounding," in *2016 10th European Conference on Antennas and Propagation (EuCAP)*, April 2016, pp. 1–5.

[10] T. Rahim, "Directional pattern synthesis in circular arrays of directional antennas," Ph.D. dissertation, University College London - Department of Electronic and Electrical Engineering, Torrington Place, August 1980.

[11] T. Rahim and D. E. N. Davies, "Effect of directional elements on the directional response of circular antenna arrays," *Microwaves, Optics and Antennas, IEE Proceedings H*, vol. 129, no. 1, pp. 18–22, February 1982.

[12] J. Hejselbæk, W. Fan, and G. F. Pedersen, "Ultrawideband vna based channel sounding system for centimetre and millimetre wave bands," in *2016 IEEE 27th Annual International Symposium on Personal, Indoor, and Mobile Radio Communication (PIMRC)*, September 2016.

[13] H. Hashemi, "The indoor radio propagation channel," *Proceedings of the IEEE*, vol. 81, no. 7, pp. 943–968, Jul 1993.